J. Membrane Biol. 80, 201–219 (1984)

The Journal of
Membrane Biology

Effects of Antidiuretic Hormone on Cellular Conductive Pathways in Mouse Medullary Thick Ascending Limbs of Henle: I. ADH Increases Transcellular Conductance Pathways

Steven C. Hebert*, Peter A. Friedman*, and Thomas E. Andreoli
Division of Nephrology, Department of Internal Medicine, University of Texas Medical School, Houston, Texas

Summary. This paper reports experiments designed to assess the relations between net salt absorption and transcellular routes for ion conductance in single mouse medullary thick ascending limbs of Henle microperfused *in vitro*. The experimental data indicate that ADH significantly increased the transepithelial electrical conductance, and that this conductance increase could be rationalized in terms of transcellular conductance changes. A minimal estimate (G_c^{min}) of the transcellular conductance, estimated from Ba^{++} blockade of apical membrane K^+ channels, indicated that G_c^{min} was approximately 30–40% of the measured transepithelial conductance. In apical membranes, K^+ was the major conductive species; and ADH increased the magnitude of a Ba^{++}-sensitive K^+ conductance under conditions where net Cl^- absorption was nearly abolished. In basolateral membranes, ADH increased the magnitude of a Cl^- conductance; this ADH-dependent increase in basal Cl^- conductance depended on a simultaneous hormone-dependent increase in the rate of net Cl^- absorption. Cl^- removal from luminal solutions had no detectable effect on G_e, and net Cl^- absorption was reduced at luminal K^+ concentrations less than 5 mM; thus apical Cl^- entry may have been a $Na^+,K^+,2Cl^-$ cotransport process having a negligible conductance. The net rate of K^+ secretion was approximately 10% of the net rate of Cl^- absorption, while the chemical rate of net Cl^- absorption was virtually equal to the equivalent short-circuit current. Thus net Cl^- absorption was rheogenic; and approximately half of net Na^+ absorption could be rationalized in terms of dissipative flux through the paracellular pathway. These findings, coupled with the observation that K^+ was the principal conductive species in apical plasma membranes, support the view that the majority of K^+ efflux from cell to lumen through the Ba^{++}-sensitive apical K^+ conductance pathway was recycled into cells by $Na^+,K^+,2Cl^-$ cotransport.

Key Words renal tubule transport · medullary thick ascending limb · ADH · K^+ conductance · Na^+,K^+,Cl^- cotransport · cell conductance

Introduction

This paper reports experiments designed to assess the relations between net salt absorption and transcellular routes for ion conductance in single medullary thick ascending limbs of Henle (mTALH). A number of groups (Hall & Varney, 1980; Sasaki & Imai, 1980; Hebert, Culpepper & Andreoli, 1981*a–c*) have noted that, in the mouse mTALH, ADH increased V_e and net Cl^- absorption (J_{Cl}^{net}) simultaneously. It was also found (Hebert et al., 1981*a*) that V_e and J_{Cl}^{net} were either reduced or abolished by 10^{-4} M luminal furosemide, by luminal omission of Na^+ or Cl^-, and by either peritubular K^+ omission or peritubular ouabain (10^{-3} M) addition. Furthermore, analogues of cyclic adenosine monophosphate (cAMP) increased V_e and accelerated J_{Cl}^{net} in a manner comparable to that observed with ADH (Sasaki & Imai, 1980; Hebert et al., 1981*a*). The above data were compatible with the possibility (Hebert et al., 1981*a,b*) that Cl^- transport in the mouse mTALH involved a furosemide-sensitive apical membrane Na^+/Cl^- cotransport process, and that ADH, operating via cAMP, accelerated the rate of net salt absorption.

It was also noted (Hebert et al., 1981*a*) that the isolated mouse mTALH paracellular pathway was predominantly Na^+-permselective. The transepithelial tracer conductance (G_t, mS cm^{-2}) computed from the sum of passive $^{22}Na^+$ and $^{36}Cl^-$ fluxes, was approximately 20 mS cm^{-2}, while the electrically measured conductance (G_e, mS cm^{-2}) was approximately 90 mS cm^{-2}. Two possibilities were cited (Hebert et al., 1981*a*) as explanations for the fact that G_e exceeded G_t: junctional complexes of the mouse mTALH might have contained single-file channels for passive $^{22}Na^+$ or $^{36}Cl^-$ permeation; and/or a fraction of transepithelial current might have traversed a cellular rather than a paracellular route.

There are several sets of observations which bear directly on the arguments and uncertainties indicated above. First, Rehm and his colleagues (Jacobson, Schwartz & Rehm, 1965; Pacifico et al.,

* Established Investigator of the American Heart Association

1969) found that addition of Ba^{++} to solutions bathing the nutrient membranes of frog gastric mucosa significantly increased transepithelial electrical resistance in that tissue, and that increasing K^+ concentrations in the nutrient solutions reversed the Ba^{++} effect. Kidder and Rehm (1970) deduced that this response of frog gastric mucosa to Ba^{++} was referable to a transcellular resistance effect. Furthermore, such Ba^{++}-sensitive apical membrane K^+ conductances have been identified in various renal diluting segments, including the early distal tubule of *Amphiuma* kidney (Guggino, Stanton & Giebisch, 1982), the rabbit cTALH (Greger & Schlatter, 1983*a*) and the rabbit cortical collecting duct (O'Neil, 1983; Koeppen, Biagi & Giebisch, 1983).

Second, there is considerable evidence that Na^+/Cl^- cotransport processes may require K^+. Geck et al. (1980) proposed an electroneutral $Na^+/K^+/Cl^-$ cotransport system for Ehrlich ascites cells, and comparable cotransport mechanisms have been noted in certain erythrocytes (Dunham, Stewart & Ellory, 1980; Palfrey, Feit & Greengard, 1980). Greger (1981*a*) and Greger and Schlatter (1983*a*) proposed that apical membrane NaCl entry in the rabbit cTALH involved an electroneutral $1Na^+/1K^+/2Cl^-$ cotransport process; a similar, but charged, $Na^+/K^+/Cl^-$ cotransport mechanism has been proposed for apical membrane NaCl entry in the intestine of the winter flounder, *Pseudopleuronectus americanus* (Halm, Krasne & Frizzell, 1982; Field, Kimberg, Orellana & Frizzell, 1982). Eveloff and Kinne (1983), working with apical membrane vesicles from rabbit mTALH, found that furosemide-sensitive coupled Na^+/Cl^- entry did not require K^+; but in other experiments with the same apical vesicles and using increased Cl^- concentrations, these workers also found that bumetanide-sensitive coupled Na^+/Cl^- uptake was enhanced by K^+.

Significantly, in both the isolated rabbit cTALH and the winter flounder intestine, an apical membrane Ba^{++}-sensitive K^+ conductance has been found to occur in parallel with the proposed $Na^+/K^+/Cl^-$ apical cotransport systems (Greger & Schlatter, 1983*a*; Halm et al., 1982). Consequently, Greger (1981*a*) suggested that, in the rabbit cTALH, the parallel arrangement of an apical membrane $Na^+/K^+/2Cl^-$ cotransport system and an apical membrane K^+ conductance provided a means for K^+ recycling across apical membranes.

Third, there are partially divergent views concerning the mode of Cl^- exit across basolateral membranes in renal tubular diluting segments. Greger and coworkers (Murer & Greger, 1982; Greger & Schlatter, 1983*b*) proposed that, in the rabbit cTALH, Cl^- transport across basolateral membranes involved both a neutral KCl efflux mechanism (similar to that observed in basolateral membranes of *Necturus* proximal tubules [Shindo & Spring, 1981]) and a Cl^--conductive exit step. Alternatively, Oberleitner, Guggino and Giebisch (1982) proposed that Cl^- exit across the basolateral membrane of the early distal tubule of *Amphiuma* was primarily conductive.

Given these considerations, we evaluated, in the mouse mTALH, the effects of ADH on transcellular conductive pathways, the relations among chemically determined net fluxes of K^+ and Cl^- and the equivalent short-circuit current, and the K^+ requirement for apical membrane NaCl entry. The electrical measurements were carried out with a refined system capable of detecting relatively small electrical conductance changes in these tubules. The experimental data indicate that ADH significantly increased the transepithelial electrical conductance, and that this conductance increase could be rationalized in terms of transcellular conductance changes. In apical membranes, K^+ was the major conductive species, and ADH directly increased the magnitude of a Ba^{++}-sensitive K^+ conductance under conditions where net Cl^- absorption was nearly abolished. In basolateral membranes, ADH increased the magnitude of a Cl^- conductance, but this ADH-dependent increase in basal Cl^- conductance depended on a simultaneous hormone-dependent increase in the rate of net Cl^- absorption.

Finally, in the companion paper, we propose a model which accounts in part for the simultaneous effects of ADH-mediated increases in V_e, G_e and net Cl^- absorption (Hebert & Andreoli, 1984). Preliminary accounts of these findings were published previously (Hebert, Friedman & Andreoli, 1982, 1983).

Materials and Methods

The basic techniques used in this laboratory for dissecting and perfusing medullary thick ascending limbs from mouse kidney have been described in detail previously (Hebert et al., 1981*a*). These general techniques were employed in the present studies. We also utilized a number of modifications, particularly in solution composition and in electrical measurements, which will be described in detail below.

In brief, 20–30 day old (~20–30 g) male Swiss white mice (Timco, Houston, TX) were sacrificed by cervical dislocation, decapitated, and rapidly exsanguinated. The kidneys were removed, sectioned into quarters by making mid-longitudinal and mid-coronal sections, and then immersed in cold (0–5°C) HEPES (N-2 hydroxyethylpiperazine-N'-2-ethanosulfonic acid)-buffered normal bathing solution (*see* below). 0.3–1.0 mm segments of medullary thick ascending limbs were dissected freehand from

the outer medullary area (*see* Hebert et al., 1981*a*, for details). Following transfer to a thermoregulated plastic chamber fitted to the stage of an inverted microscope, the tubule segments were mounted between two sets of concentric pipettes and perfused at rates between 5–20 nl/min, depending on the experimental protocol. During perfusion, temperature was maintained at 37 ± 0.5°C.

Composition of Solutions

For routine experiments, we used a standard HEPES-buffered solution containing (mM): 140 NaCl, 5.0 KCl, 1.0 $CaCl_2$, 1.2 $MgCl_2$ and 3.0 HEPES. HEPES was used as a buffer in the present experiments to avoid anions that might form precipitates with Ba^{++}. The perfusing and bathing solutions were identical except for the addition of 5.5 mM glucose and 0.4 g/100 ml of exhaustively dialyzed bovine serum albumin (BSA, Fraction V, Reheis Chemical Co., Phoenix, AZ) to bathing solutions, and an equiosmotic concentration of urea to perfusion solutions. All solutions were adjusted to an osmolality of 300 mOsm/kg H_2O and a pH of 7.40 after equilibration with 100% O_2. (CO_2 + HCO_3^-) were not included in external solutions, since both basal and ADH-dependent NaCl transport are unaffected by the presence or absence of (CO_2 + HCO_3^-) (Hebert et al., 1981*a*). Chloride-free solutions were made by replacing NaCl isosmotically with Na-isethionate. Barium, where indicated, was added to the perfusate in the form of $BaCl_2$. No ion substitutions were made in the bath for perfusate $BaCl_2$ additions or in the perfusate for KCl removal, since such differences in ionic composition of the perfusate and bath produced negligible dilution voltages (<0.5 mV).

ADH (synthetic arginine vasopressin, Grade V, Sigma Chemical Co., St. Louis, MO), where indicated, was added to peritubular media at 10 μU/ml, a concentration that produces a maximal increase in transepithelial voltage and in the rate of NaCl absorption from the mouse mTALH (Hebert et al., 1981*a*,*b*). Furosemide was kindly provided by Hoechst Pharmaceuticals, Somerville, NJ.

Prostaglandin E_2 (PGE_2) was obtained from Sigma Chemical Co. As described previously (Culpepper & Andreoli, 1983), PGE_2 was reconstituted in 95% ethanol, stored at −20°C, and added to the bath immediately prior to an experiment. In the present experiments (cf. Fig. 9), we added 10^{-6} M PGE_2 to bathing solutions; the latter concentration is tenfold greater than that required for maximal inhibition of the ADH-dependent values of net Cl^- absorption and spontaneous transepithelial voltage (Culpepper & Andreoli, 1983). The dibutyryl analogue (db-cAMP) of cyclic adenosine monophosphate (Sigma Chemical Co.) was stored at −40°C and added to bathing solutions immediately prior to each experiment as described previously (Hebert et al., 1981*a*; Culpepper & Andreoli, 1983).

Microchemical Determinations

Potassium concentrations in samples of perfusate or collected fluid were measured using a graphite furnace atomic absorption spectrophotometer (Instrumentation Laboratory Model 951/655, Instrumentation Laboratory, Wilmington, MA) following the general procedure outlined by Good and Wright (1979). An aliquot of tubular fluid, approximate volume 20 nl, was deposited on a pyrolytically coated graphite microboat and loaded into the spectrophotometer. The furnace was then heated to 2300°C and the signal transient during atomization was quantified by peak height. A monochromatic hollow cathode light source (1L Model 62863) was used, and the absorption was read at 7699 Å. The coefficient for determination of replicates was between 2–4%. The analysis was linear for K^+ concentrations in the range 0–8 mM, with a regression coefficient 0.99 and a 2% variation in slope.

Since the presence of sodium in the analysate resulted in some quenching of the incident light, all of the potassium standard solutions contained 150 mM NaCl. No significant difference in the extent of quenching was observed in the range of 80–150 mM NaCl, that is, over the NaCl concentration range normally seen in collected fluid samples during either ADH-independent or ADH-dependent net Cl^- absorption (Hebert et al., 1981*b*). Since the rate of net fluid absorption in the mouse mTALH is negligible (Hebert et al., 1981*a*), J_K^{net} (pmol sec^{-1} cm^{-2}), the net potassium flux, was computed as

$$J_K^{net} = \frac{\dot{V}_o([K^+]_o - [K^+]_l)}{A} \quad (1)$$

where $\dot{V}_o$ is the perfusion rate, $[K^+]_o$ and $[K^+]_l$ are the concentrations of potassium in perfused and collected fluid samples, respectively, and A is the surface area, computed from the dimensions of the segment measured with an eyepiece micrometer.

The chloride concentrations in aliquots of perfused and collected samples of tubular fluid were determined in triplicate using the electrotitrametric procedure described by Ramsey, Brown and Croghan (1955). Net chloride absorption (J_{Cl}^{net}, pmol sec^{-1} cm^{-2}) was calculated according to the following relation:

$$J_{Cl}^{net} = \frac{\dot{V}_o([Cl^-]_o - [Cl]_l)}{A} \quad (2)$$

where $[Cl]_o$ and $[Cl]_l$ refer to the chloride concentrations in perfused and collected fluid samples, respectively.

In order to make optimal the sensitivities of net fluxes determined chemically, we used the longest tubule lengths technically attainable. In the present studies, the mean tubule length for net flux determinations was 0.8 ± 0.2 mm (n = 33).

Tracer Fluxes

The unidirectional bath-to-lumen flux of sodium was determined as described previously (Hebert et al., 1981*a*) by the addition of $^{22}NaCl$ (carrier free; New England Nuclear, Boston, MA) to the bathing solution at an average concentration of 7.0×10^{-11} cpm/mol. $^{22}Na^+$ activity in the bath was measured at the beginning and end of each tubular fluid sampling period. No significant change in bath isotope activity was discernible during this interval. To avoid appreciable $^{22}Na^+$ accumulation in luminal fluid, we used relatively high perfusion rates, 16.4 ± 1.2 nl/min, in these experiments. Under these conditions, the $^{22}Na^+$ concentration (Eq. (3)) of the collected fluid sample was uniformly less than 5% of that in the bathing solution.

The ionic permeability coefficient for sodium (P_{Na}, cm sec^{-1}) was computed as described previously (Schafer, Troutman & Andreoli, 1974; Hebert et al., 1981*a*) from the expression

$$P_{Na} = \frac{\dot{V}_o^*[^{22}Na^c]RT}{AV_eFX_{Na}^b} \frac{1 - \exp\left(\frac{FV_e}{RT}\right)}{C_{Na}^b} \quad (3)$$

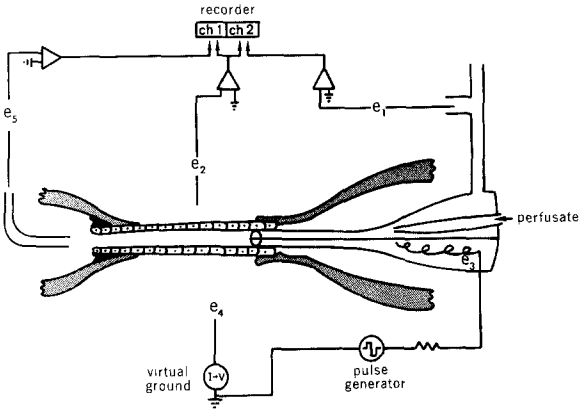

Fig. 1. Schematic representation of the *in vitro* tubule perfusion setup modified for electrical measurements. The electrical connections e_1–e_5 are described in detail in Methods

where F, R, and T have their usual meaning, $*[^{22}Na^c]$ is the tracer concentration of sodium in the collected fluid samples, C^b_{Na} (mol cm^{-3}) is the concentration of Na^+ in the bathing solution, and X^b_{Na} (cpm mol^{-1}) is the activity of $^{22}Na^+$ in the bath.

Electrical Measurements

In our earlier studies (Hebert et al., 1981*a–c*), V_e and G_e were measured using a single axial luminal electrode, so that the latter served simultaneously as a current-passing and voltage-sensing electrode. In the present experiments, we wished to improve the precision of conductance measurements significantly in order to detect, with confidence, conductance changes of about 10 mS cm^{-2} in tubules having total transepithelial conductances in the range of 80–150 mS cm^{-2}. Accordingly, the electrical system was modified, following Greger (1981*b*), to provide separate electrodes for passing current and reading voltage, both in luminal fluids and in the bath; and all comparisons were carried out by making paired observations on individual tubules.

The electrical circuit used for V_e and G_e measurements is shown schematically in Fig. 1. The perfusion pipette was modeled after that described by Greger (1981*b*), and was formed from 2-mm electrode glass that was divided in half axially by a glass septum (theta-glass). One half of the theta-glass pipette was used to perfuse the tubule and was fitted with an exchange pipette (PE10 tubing tapered at one end) through which perfusate was continuously flushed at a rate of approximately 5 ml/min. This allowed the perfusion solution to be changed without altering tubular pressure or flow; exchanges were complete in less than 30 sec. Perfusate flow rate, sustained by both hydrostatic and air pressure, was maintained at 10–20 nl/min so that axial changes in perfusate ion concentrations were negligible (Hebert et al., 1981*b*) and the spontaneous transepithelial voltage was chemically clamped along the length of the tubule.

The other half of the theta-glass perfusion pipette formed the current-passing limb, and was fitted with a Ag/AgCl wire (e_3, Fig. 1) and a fluid exchange system (0.01″ ID, 0.03″ OD Microline tubing pulled to the appropriate size) through a hole drilled in the back of the pipette. This side was electrically sealed from the perfusion side, at the back, with a low viscosity epoxy. The fluid exchange system permitted fresh 0.9% NaCl to be introduced into the current-passing limb prior to each experiment.

Biphasic square wave current pulses, 400–500 nA in magnitude and approximately 800 msec in duration; were produced by two anapulse stimulators (W-P Instruments, New Haven, CT, Model 301) connected to stimulus isolators (W-P Instruments Model 305) and were passed via the Ag/AgCl wire, e_3 in Fig. 1, into the tubule lumen. The current ground loop, e_4 in Fig. 1, was formed by a Ag/AgCl wire inserted into the bath and connected to a virtual ground (current-to-voltage converter, W-P Instruments Model 180).

The transepithelial voltage (lumen with respect to bath) was measured between the perfusion half of the perfusion pipette (e_1 in Fig. 1) and the bath (e_2 in Fig. 1), using a high impedence ($\cong 10^{15}$ Ω) differential amplifier (W-P Instruments, Model F223A). Electrical connections were made to the perfusate and bathing solutions via free-flowing KCl-Ag/AgCl bridges (W-P Instruments MERE-1 reference, microelectrode) filled with 3 M KCl. Since these were at the outflow ends of the perfusion and bathing systems, the tubule was chemically isolated from these bridges. No liquid-junction corrections were necessary with this system. Voltage at the collecting end was measured with a 4% agar/0.9% NaCl-filled electrode joined to a calomel half-cell (e_5 in Fig. 1) and connected to a high impedence electrometer ($\cong 10^{13}$ Ω), and was read differentially between e_5 and e_2 (Fig. 1). Since only imposed voltage changes were necessary to calculate G_e, the collecting-end electrode was not zeroed and any liquid junctions were ignored.

The transepithelial electrical conductance was calculated as before (Hebert et al., 1981*a*) using cable equations described previously (Burg, Isaacson, Grantham & Orloff, 1968; Helman, 1972; Helman, Grantham & Burg, 1971; Lutz, Cardinal & Burg, 1973). As will be indicated below, we used relatively short tubule lengths, generally less than 0.3 mm, for electrical conductance measurements. The theta-glass perfusion system produced very stable baseline voltage deflections of less than 4–5 mV for 400–500 nA current pulses, and represented less than 10% of the total voltage deflection at the perfusion end when a tubule was in place.

Figure 2 shows the typical voltage responses at the perfusion end of the isolated mTALH to an 800 sec biphasic current pulse. The positive current pulses were directed from lumen to bath, and the negative current pulses from bath to lumen. In most tubules under control conditions (*see* first and third biphasic deflections in Fig. 2), the voltage deflection in either the positive or negative direction did not reach a plateau or steady-state value but continued to polarize. This type of response, termed the "long time-constant" response by Kidder and Rehm (1970), also appears to be characteristic of isolated rabbit renal tubules (Koeppen et al., 1983; O'Neil, 1983). The simultaneous addition of 5 mM Ba^{++} and K^+ removal from the perfusate decreased G_e and concomitantly abolished this polarization effect (*see* second biphasic pulse in Fig. 2). This finding thus confirms the results of Kidder and Rehm (1970), who pointed out that, in frog gastric mucosa, the increase in transepithelial resistance produced by Ba^{++} in nutrient solutions also resulted in abolition of the long time-constant response.

All voltage deflections were read from a strip chart recorder (Gould 2200S Recorder, Gould, Inc., Cleveland, OH) at 100–150 msec after onset of the current pulse, since any pipette and tubule capacitance changes were presumably complete at this time. The magnitude of the voltage deflection in each direction used in the cable analysis was obtained by subtracting the baseline deflection in the absence of a tubule (*see* above) from that measured in the presence of a tubule.

A comparison of the optical tubule diameter measured from micrographs at 200× and that calculated from the cable equa-

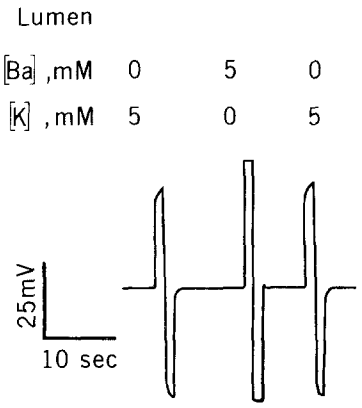

Fig. 2. Perfusion-end voltage deflections across the mouse mTALH resulting from biphasic square-wave current pulses. The first and third transepithelial voltage deflections were obtained under control conditions (5 mM K^+ and 0 mM Ba^{++} in lumen) and the middle transepithelial voltage deflection with 0 mM K^+, 5 mM Ba^{++} in the lumen. For the control condition, the voltage deflections did not reach steady-state peaks but continued to polarize with time (the long time-constant effect described by Kidder and Rehm [1970]). The middle voltage deflection demonstrates, in accord with the results of Kidder and Rehm (1970), ablation of the long time constant effect with simultaneous K^+ removal and 5 mM Ba^{++} addition to luminal fluids; the third voltage deflection shows that the long time constant reappeared when control conditions were re-established

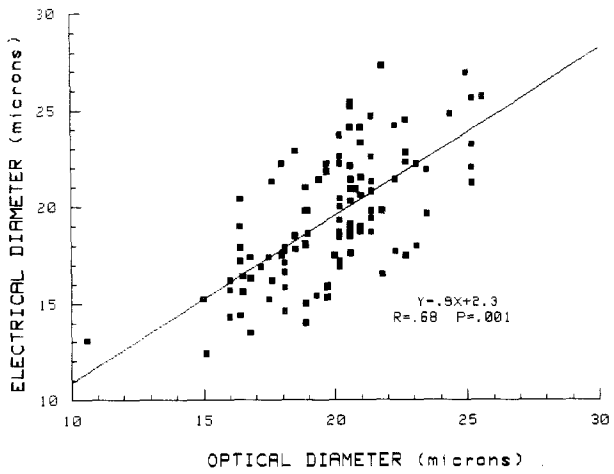

Fig. 3. Relation between the measured geometric tubule diameter (optical diameter) and that calculated from cable analysis (electrical diameter) in the mouse mTALH. Each point represents a measurement in an individual tubule (n = 111). The line represents the least-squares regression of the data: y = (0.86 ± 0.14)x + (2.3 ± 0.2); r = 0.68 ($P < 0.001$).

tions, for more than 100 tubules, is shown in Fig. 3. Clearly, there was a highly significant linear correlation between these two diameters with a slope that did not differ from unity. Thus there was an excellent correlation between optical and electrical radii, although certain tubules exhibited considerable scatter. To avoid experimental bias, all the tubules shown in Fig. 3 were used in the present experiments, and evaluation of the effect of a given maneuver on G_e involved only paired comparisons.

Measurement of the Equivalent Short-Circuit Current, J_e

Direct measurement of the short-circuit current by voltage clamping via an axial wire along the entire length of the tubule was not feasible technically for these mTALH segments, because the latter were electrically leaky and had small luminal volumes. However, for symmetrical perfusion and bathing solutions, an equivalent short-circuit current (I_{sc}, A cm^{-2}) or equivalent ionic flux (J_e, pEq sec^{-1} cm^{-2}), can be calculated from Ohm's law, using the spontaneous open-circuit transepithelial voltage and the measured value of G_e, as (Schultz, Frizzell & Nellans, 1977)

$$J_e = I_{sc}/F = \frac{V_e G_e}{F}. \tag{4}$$

We used this approach, described originally by Greger (1981*b*) for the *in vitro* microperfused rabbit cTALH, for equivalent short-circuit measurements in the mouse mTALH.

All measurements of J_e were made at perfusion rates between 10–20 nl min^{-1}, when the tubules were essentially chemically and voltage clamped, that is, the perfusate ionic concentrations, and hence V_e, changed negligibly along the axial length of the tubule (Hebert et al., 1981*a–c*). Furthermore, because of the short length constant of these tubule segments (0.096 ± 0.002 mm; +ADH, n = 85; and 0.100 ± 0.012 mm; −ADH, n = 26), we used relatively short tubule lengths for J_e measurements. In the present studies, the mean tubule length for J_e and G_e determinations was 0.24 ± 0.01 mm (n = 111).

Salt Dilution Voltages

Sodium-to-chloride permselectivity ratios (P_{Na}/P_{Cl}) were determined as described previously (Hebert et al., 1981*a*) from the measurement of zero-current salt-dilution voltages at zero volume flow (J_v = 0) produced by transepithelial ion activity gradients according to the Goldman-Hodgkin-Katz equation:

$$V_e = \frac{2.3\,RT}{F} \log \left[\frac{(P_{Na}/P_{Cl})\alpha^b_{Na} + \alpha^l_{Cl}}{(P_{Na}/P_{Cl})\alpha^l_{Na} + \alpha^b_{Cl}} \right] \tag{5}$$

where α^b and α^l are the ion activities in bathing and perfusing solutions, respectively. As indicated previously (Hebert et al., 1981*a*), liquid junction voltages were insignificant since the voltages were measured with respect to 3 M KCl-Ag/AgCl bridges. The activity coefficients of Na^+ and Cl^- in each solution were calculated as described previously (Hebert et al., 1981*a*) from the Debye-Huckel law (Salling & Siggaard-Anderson, 1971) using the ion size parameters published by Kielland (1937).

Statistical Analyses

Four to eight current injections were performed for each experimental condition in a given tubule, and a resistance value was calculated for each injection. The average of these values provided the mean value for that tubule for that condition. These

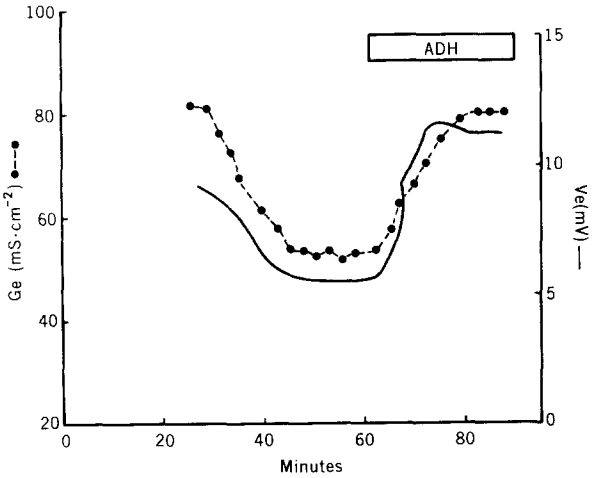

Fig. 4. Representative experiment illustrating the effect of ADH on transepithelial electrical conductance, G_e, and on the spontaneous transepithelial voltage, V_e, in mouse mTALH. The tubule was perfused at 37°C in control solutions in the absence of bath ADH. After V_e and G_e reached ADH-independent steady-state nadir values, ADH (10 μU/ml) was added to the bath

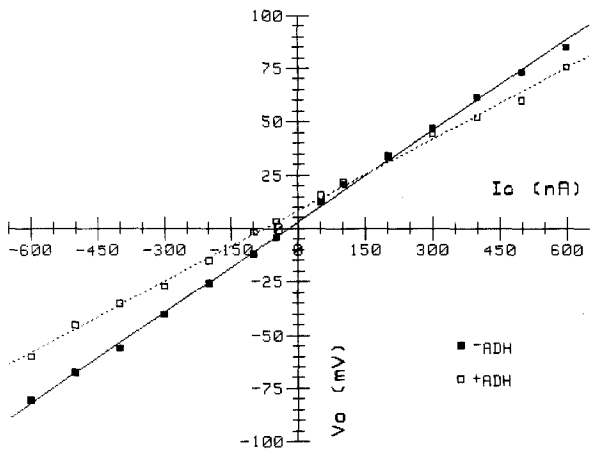

Fig. 5. A representative experiment illustrating the current-voltage relations in a single mTALH segment with (open squares connected by a dashed line) and without ADH (closed squares connected by a solid line)

average values from a number of tubules were used to compute a mean ± standard error of the mean (SEM) for the indicated number of tubules (n). Statistical significance for mean paired differences was evaluated by the student t test and probabilities (P) were computed from the t distribution with significance being <0.05. A Hewlett-Packard 9845B computer was used to perform all calculations and to generate some of the graphs used in this report.

Results

Effect of ADH on Transepithelial Conductance

Figure 4 shows the results of a representative experiment illustrating the protocol for evaluating the effects of ADH on V_e and G_e. The G_e values were obtained at 2–3 min intervals and are connected by dashed lines; V_e, shown as the solid curve, was read continuously; and the zero time was taken to be the time of animal sacrifice. At 20 min, tubule perfusion was begun in the absence of bath ADH; over the next 20 min, G_e and V_e decreased monotonically to steady-state values of 53 mS cm^{-2} and 5.5 mV, respectively. At 60 min, ADH (10 μU/ml) was added to the bath and, after a 60–90 sec delay, G_e and V_e increased monotonically to steady-state values of 80 mS cm^{-2} and 11.2 mV, respectively. During the steady-state periods, either with or without hormone, G_e varied by less than 2–3 mS cm^{-2} between current pulses.

The results in Fig. 4 confirm our earlier observations (Hebert et al., 1981*a*) on the effect of ADH on V_e, and show that ADH increased G_e *pari passu* with increasing V_e. Two other results, not shown in Fig. 4, are also noteworthy. First, in experiments in which ADH was present in the bath from zero time, there was no detectable temporal decline in either V_e or G_e. Second, in experiments where ADH was not added to the bath, G_e and V_e were constant with respect to time after having reached a nadir. Accordingly, as in prior studies (Hebert et al., 1981*a–c*), we took the steady-state nadir values of V_e and G_e, when ADH was absent from the bath, to represent ADH-independent values.

The current-voltage relations for a single perfused mTALH segment both with (open squares connected by a dashed line) and without (solid squares connected by a solid line) ADH are shown in Fig. 5. Both current-voltage relations were clearly linear ($r > 0.99$, $P < 0.0001$) over the range of current pulses from −600 to +600 nA; therefore, single current pulses within this range were adequate to determine G_e. Moreover, it is evident from Fig. 5 that ADH (10 μU/ml) both increased V_e (Y-intercept) from 4.1 to 9.4 mV and reduced the input resistance (i.e., slope of the current-voltage relation) from 1.42×10^5 to 1.11×10^5 Ω. The transepithelial conductances calculated from these input resistances were 92.8 mS cm^{-2} and 118.8 mS cm^{-2}, without and with hormone, respectively.

Figure 6 presents the results of experiments involving paired measurements of G_e with and without ADH. The ADH-independent and ADH-dependent conductances used in this figure correspond to the steady-state values defined for these conditions in Fig. 4. The data shown in Fig. 6 indicate that bath

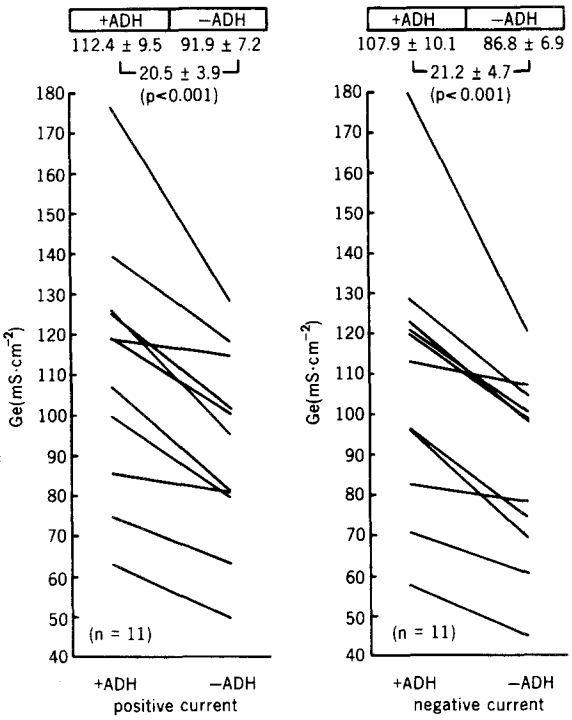

Fig. 6. The effect of ADH (10 U/ml in the bath) on transepithelial conductance, G_e, in paired experiments using both positive currents (left-hand panel) and negative currents (right-hand panel). mTALH tubules were perfused at 37°C in symmetrical control solutions. Each line connects measurements in an individual tubule. The results are expressed as mean values ± SEM

ADH (10 μU/ml) produced an increase in G_e of approximately 20 mS cm^{-2}; for the eleven tubules shown in Fig. 6, ADH also increased V_e from 5.7 ± 0.7 to 10.7 ± 1.0 mV, a result virtually identical to that reported previously (Hebert et al., 1981*a*).

In earlier studies, it was reported (Hebert et al., 1981*a*) that ADH did not appear to significantly affect the transepithelial electrical resistance of the mTALH, a result which differs from the data shown in Fig. 6. This discrepancy between previous results and those presented in Fig. 6 may relate to at least two factors. In the present studies, the electrical system contained separate pairs of electrodes for passing current and reading voltage, both in lumen and bath (Fig. 1), while the prior electrical data were obtained using single electrodes in lumen and bath for passing current and reading voltage. Second, the previous results (Hebert et al., 1981*a*) on the lack of effect of ADH on G_e depended on an unpaired group comparison among 5 tubules; and given the wide variation among G_e values for a given condition (*see* Fig. 6), the tubule number may have been inadequate to detect significant G_e differences between ADH-dependent and ADH-independent cases. It is therefore relevant to note that, for

Table 1. Effect of Cl$^-$ omission in perfusate or bath on the ADH-dependent G_e

Perfusate Cl$^-$	Bath Cl$^-$	G_e	ΔG_e (Cl$^-$ omission)
(mM)		(mS cm^2)	
145	145	112.7 ± 15.5	1.6 ± 4.4
0	145	111.1 ± 13.8	(NS)
		(n = 5)	
145	145	126.7 ± 18.5	24.6 ± 5.3
145	0	102.1 ± 17.1	($P < 0.01$)
		(n = 5)	

Two sets of experiments were carried out measuring G_e using positive luminal currents for each experimental condition in each tubule. In the upper set of experiments, Cl$^-$ was replaced isosmotically with isethionate in the perfusate. In the lower set of experiments, isethionate replaced bath Cl$^-$. ΔG_e refers to the mean paired difference between the control conductance and that measured when Cl$^-$ was omitted either from perfusate or bath. ADH, 10 μU/ml, was uniformly present in bathing solutions. The data are expressed as mean values ± SEM.

all the tubules reported in the present experiments, the unpaired values of G_e were: without ADH, 89.3 ± 5.5 mS cm^{-2} (n = 26); with ADH, 117.3 ± 3.9 mS cm^{-2} (n = 85); and that the unpaired mean difference between these values, 28.0 ± 7.7 mS cm^{-2}, was highly significant ($P < 0.001$).

It is obvious that the transepithelial conductance G_e in these mouse mTALH segments is the sum of two parallel conductance elements: G_s, the conductance through the paracellular pathway; and G_c, the conductance through the cellular pathway. Consequently, additional experiments were carried out to evaluate whether the ADH-dependent increase in G_e was referable to hormone-induced changes in G_s and/or G_c.

Evaluation of Cl$^-$ Conductive Pathways

Effect of Removing Cl$^-$ from External Solutions on G_e

Table 1 shows the results of two sets of paired measurements on G_e in which Cl$^-$ in either luminal or peritubular solution was replaced isosmotically with isethionate; ADH, 10 μU/ml, was present in all bathing solutions. In all instances, G_e values with Cl$^-$ omission were bracketed with pre- and post-control G_e measurements with Cl$^-$ in luminal and bathing solutions. Thus the control G_e values for a given tubule represent the mean of G_e measurements at the beginning and end of a given experi-

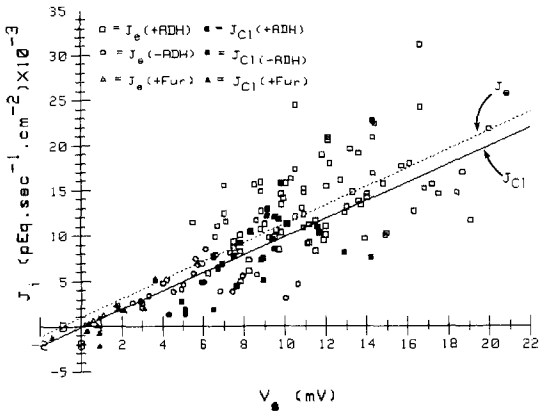

Fig. 7. The relations between net Cl^- absorption determined chemically (J_{Cl}^{net}, denoted in this figure as J_{Cl}), the equivalent short-circuit current J_e, and the spontaneous transepithelial voltage V_e. J_e (open symbols) and J_{Cl} (closed symbols) values for individual tubules were plotted with their simultaneously measured V_e values for the following conditions: with (+ADH) or without (−ADH) antidiuretic hormone (10 μU/ml in the bath); and in the presence of 10^{-4} M luminal furosemide (+Fur) with ADH present in the bath. The lines on the graph represent least squares linear regressions of J_{Cl} versus V_e (solid line, $J_{Cl} = (1.00 \pm 0.6)\ V_e + (0.09 \pm 0.01)$, $r = 0.92$; and of J_e versus V_e (dashed line, $J_e = (1.04 \pm 0.16)\ V_e + (0.95 \pm 0.06)$, $r = 0.78$

ment. The values of G_e were computed from the voltage deflection produced from positive luminal current injections (*see* Methods); the same experimental format was utilized in the experiments reported in Tables 2 and 3.

The results in Table 1 indicate that removal of Cl^- from either luminal or peritubular fluids produced asymmetrical changes in G_e. When Cl^- was omitted from luminal fluids, G_e was reduced by approximately 1.5%, and the fall in G_e was not statistically significant. However, when Cl^- was removed from peritubular solutions, G_e fell by approximately 19.4%, and the fall in G_e was clearly significant ($P < 0.01$). We wish to emphasize that these latter data do not provide a way of assessing absolute Cl^- conductances in either apical or basolateral membranes, since the latter two membranes represent two conductance elements in series. Likewise, these data provide no direct estimate of the Cl^- conductance of the paracellular pathway, which is a conductance route in parallel with the transcellular pathway.

However, the fact that Cl^- removal from luminal solutions had a negligible effect on G_e indicates that the Cl^- conductance of apical surfaces of these tubules, including both apical membranes and the luminal faces of junctional complexes, was too small to be detected by the present experimental methods. Moreover, since Cl^- transport across these apical plasma membranes involves a furosemide-sensitive process (Hebert et al., 1981*a*; Fig. 7), the observation that Cl^- omission from luminal fluids had no significant effect on G_e (Table 1) indicates that any conductance referable to this furosemide-sensitive Cl^- entry step was rather small with respect to the total conductance of the luminal surfaces (i.e., apical membranes and the luminal faces of junctional complexes).

The data in Table 1 also indicate clearly that Cl^- removal from peritubular fluids produced a significant fall in G_e, and that the latter reduction was greater than that observed when Cl^- was removed from luminal solutions. Moreover, the ionic permeability characteristics of the paracellular pathway in these mTALH segments are symmetrical, at least for Na^+ and Cl^-, since P_{Na}/P_{Cl} ratios determined from salt dilution voltages have the same values whether calculated from luminal dilutions or bath dilutions (Hebert et al., 1981*a*). These latter observations, when coupled with the fact that luminal Cl^- omission had no detectable effect on G_e, support the argument that basolateral membranes of these tubules contained a significant Cl^- conductive pathway.

We emphasize again in this context that the fall in G_e produced by Cl^- omission from peritubular fluids, subsequently termed $\Delta G_e^{Cl_b}$, does not indicate the explicit values for either the total conductance of basolateral membranes or the Cl^- conductance of basolateral membranes. However, we may use the change in $\Delta G_e^{Cl_b}$ with different maneuvers as an index to whether such maneuvers increased, decreased, or left the basolateral Cl^- conductance unchanged.

Effect of ADH on $\Delta G_e^{Cl_b}$

Table 2 shows the effects of bath Cl^- removal on G_e and $\Delta G_e^{Cl_b}$ in the presence and absence of ADH. The control G_e data, when Cl^- was present in luminal bathing solutions, affirm the results shown in Fig. 6: when ADH was added to bathing solutions, there was a clearly discernible rise in G_e. Table 2 also shows that the value of $\Delta G_e^{Cl_b}$ was clearly greater with ADH than without ADH. Therefore, by using the value of $\Delta G_e^{Cl_b}$ as an index to the Cl^- conductance in basolateral membranes (Table 1), the results shown in Table 2 indicate that ADH increased this basolateral Cl^- conductance.

In order to evaluate the relation between ADH-mediated increases in $\Delta G_e^{Cl_b}$ and hormone-mediated increases in transcellular Cl^- transport, we assessed the effects of ADH and bath Cl^- removal on

Table 2. Effect of Cl^- removal on G_e in the presence and absence of ADH

ADH	Control G_e (bath Cl^- present)	$\Delta G_e^{Cl_b}$ (bath Cl^- removal)	
	(mS cm^{-2})		
−	84.8 ± 7.3	−19.5 ± 1.9	($P < 0.001$)
+	98.6 ± 7.7	−28.5 ± 3.2	($P < 0.001$)
Mean paired difference	13.9 ± 3.5 ($P < 0.01$)	9.0 ± 2.7 ($P < 0.001$)	
	($n = 8$)		

G_e and $\Delta G_e^{Cl_b}$ were measured as described in Table 1. $\Delta G_e^{Cl_b}$ was taken as the reduction in G_e which occurred when Cl^- was removed from bathing solutions. All experiments involved paired comparisons on individual tubules. ADH, when present, was added to the bath, 10 μU/ml. All data were expressed as mean values ± SEM.

Table 3. Effect of ADH and bath Cl^- omission on $\Delta G_e^{Cl_b}$ in the presence of 10^{-4} M luminal furosemide

Bath ADH	$\Delta G_e^{Cl_b}$
(μU/ml)	(mS cm^2)
0	−17.5 ± 1.0
10	−19.5 ± 1.0
Mean paired difference	2.0 ± 1.4 (NS)
[n = 3]	

$\Delta G_e^{Cl_b}$ was measured, as described in Tables 1 and 2, as the conductance difference which occurred when Cl^- was omitted from bathing solutions. All experiments involved paired comparisons on individual tubules. $\Delta G_e^{Cl_b}$, in each of the two circumstances, had a P value less than 0.001. The data are expressed as mean values ± SEM.

$\Delta G_e^{Cl_b}$ in the presence of 10^{-4} luminal furosemide, an agent which strikingly reduces both net Cl^- absorption and V_e (Hebert et al., 1981*a*). Table 3 lists the $\Delta G_e^{Cl_b}$ values obtained in the presence or absence of ADH, but with 10^{-4} M furosemide present in all luminal fluids. A comparison of the results in Tables 2 and 3 indicates that 10^{-4} M luminal furosemide prevented the ADH-mediated increase in the magnitude of $\Delta G_e^{Cl_b}$. In other words, the hormone-induced increase in the magnitude of $\Delta G_e^{Cl_b}$ occurred only when ADH-mediated increments in net Cl^- absorption were not blocked.

Relation between J_e and J_{Cl}

Another way of evaluating Cl^- conductive pathways in basolateral membranes was to compare the magnitudes of the equivalent ionic flux, J_e, and the chemical net Cl^- flux, J_{Cl}^{net}, under a variety of conditions. Technical constraints precluded paired measurements of J_e and J_{Cl}^{net} in the same tubule since, for maximal accuracy, J_e and J_{Cl}^{net} were measured in relatively short and relatively long tubule segments, respectively. However, both with and without ADH, there is a close relation between the magnitude of V_e and the magnitude of J_{Cl}^{net} (Hebert et al., 1981*a*). Therefore in the present experiments, we compared the relations between J_{Cl}^{net} and V_e and J_e and V_e.

Figure 7 shows the results of a large number of such experiments. Each point represents a single tubule. J_e measurements were made on tubule segments averaging 0.24 ± 0.01 mm in length ($n = 111$ tubules) and at perfusion rates in the range 12–16 nl min^{-1}, so that the Cl^- concentration of tubular fluid varied negligibly between perfused and collected fluid (Hebert et al., 1981*b*). The J_{Cl}^{net} measurements were made on tubule segments averaging 0.8 ± 0.2 mm ($n = 33$ tubules) in length. Since J_{Cl}^{net} in these tubules increases monotonically with perfusion rate, the perfusion rate in each net Cl^- flux experiment was adjusted to the maximal value consistent with a reliable determination of J_{Cl}^{net} (Hebert et al., 1981*b*). For the ADH-independent case, V_o was approximately 5 nl min^{-1}; and for the ADH-dependent case, V_o was approximately 8 nl min^{-1} (Hebert et al., 1981*b*).

The data presented in Fig. 7 indicate, in accord with earlier observations (Hebert et al., 1981*a*), that there was a close relation between J_{Cl}^{net} and V_e in the presence and absence of ADH, and when 10^{-4} M furosemide was either present or absent from luminal solutions. The relation between J_{Cl}^{net} and V_e, using all data, could be expressed by the linear equation $y = (1.00 \pm 0.06)x + (0.09 \pm 0.01)$, with a regression coefficient of 0.92. Likewise, the relation between J_e and V_e, using all data, could be expressed by the linear relation $y = (1.04 \pm 0.16)x + (0.95 \pm 0.06)$, with a regression coefficient of 0.78.

In other words, under a wide variety of conditions and for relatively large numbers of tubules, J_{Cl}^{net} was approximately 90% of J_e. Clearly, this result could obtain if most of the net transport of Cl^- across basolateral membranes were conductive. However, results identical to those shown in Fig. 7 might occur even with appreciable electroneutral net Cl^- transport across basolateral membranes if

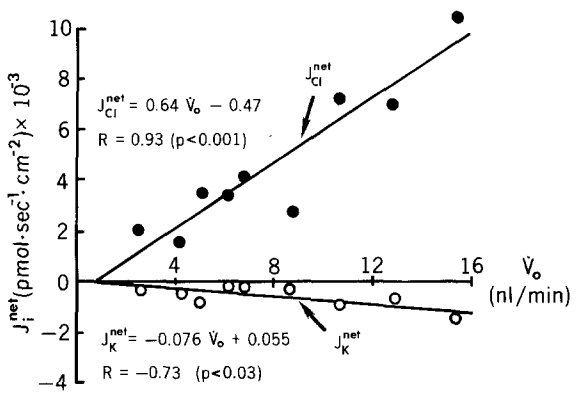

Fig. 8. Relations between net Cl^- absorption (J_{Cl}^{net}, closed circles) and net K^+ secretion (J_K^{net}, open circles) and tubule perfusion rate, V_o, in mouse mTALH. Both Cl^- and K^+ concentrations were determined, as described in Methods, on the same perfusion and collected fluid samples at each of the indicated V_o values. ADH, 10 μU/ml, was present in all bathing solutions

apical membranes contained a cation conductive pathway through which net cation secretion was sufficiently large to account for J_e. Consequently, it was prudent to evaluate the relation between net Cl^- absorption and net K^+ secretion.

The results of these experiments are presented in Fig. 8. J_{Cl}^{net} and J_K^{net} were measured simultaneously in a series of tubules. ADH was uniformly present in bathing solutions; and because J_{Cl}^{net} varies with perfusion rate in these tubules (Hebert et al., 1981*b*), the latter was varied at random to examine the relation between J_{Cl}^{net} and J_K^{net} over a range of perfusion rates. The data shown in Fig. 8 indicate, in accord with prior studies (Hebert et al., 1981*b*), that J_{Cl}^{net} increased with increasing perfusion rates. Net K^+ secretion was present, and like net Cl^- absorption, J_K^{net} also increased with perfusion rate. Furthermore, for both K^+ and Cl^-, there was a clear linear relation between J_i^{net} and V_o. Of particular importance in the present context is the fact that, either by inspection of the individual data points or by a comparison of the linear relations between J_i^{net} and V_o, the rate of net K^+ secretion was approximately 10% of the rate of net Cl^- absorption over the entire range of perfusion rates tested.

Thus the results presented in Fig. 8 are consistent with the view that net K^+ secretion contributed approximately 10% to the values of J_e reported in Fig. 7. Consequently, net Cl^- absorption, rather than net K^+ secretion, was the major component of J_e. When considered in this context, the observation that J_{Cl}^{net} was 90% of J_e (Fig. 7) supports the contention that the majority of net Cl^- transport across basolateral membranes was conductive.

Effect of Luminal Amiloride on G_e

It was not possible to assess the contribution of Na^+ to apical membrane conductance by experiments in which Na^+ was omitted from luminal fluids, since the permeability of the paracellular pathway to Na^+ is rather large (Hebert et al., 1981*a*; Table 5). However, it was noted previously that 10^{-3} M luminal amiloride had no effect on V_e, and hence presumably on J_{Cl}^{net} (Hebert et al., 1981*a*). Thus in the present experiments, we tested the effects of 10^{-3} M luminal amiloride on G_e in paired observations. The experimental protocol involved paired comparisons of G_e values in tubules under two conditions: when perfusate and bath contained standard HEPES-buffered solutions; and when 1 mM amiloride was added to luminal solutions. The G_e measurements with 10^{-3} M amiloride were bracketed with pre- and post-control measurements with standard solutions. The mean G_e value when amiloride was absent was 110 mS cm^{-2}; with 10^{-3} M amiloride in luminal solutions, the mean G_e was virtually the same, 108 mS cm^{-2}. Thus these results indicate that amiloride-sensitive apical membrane Na^+ channels made a negligible contribution to G_e.

Evaluation of Apical K^+ Conductance

Effect of Simultaneous Luminal Ba^{++} Addition and K^+ Removal on the ADH-Dependent G_e

The results presented in Fig. 8 show that apical membranes of these mTALH segments contained a K^+ secretory pathway. In order to evaluate the conductive characteristics of this pathway, we carried out paired experiments testing the effects of combined 5 mM luminal Ba^{++} addition and luminal K^+ deletion on the ADH-dependent G_e, using both positive and negative current pulses (Fig. 9). The choice of these conditions was based on the preliminary findings (Hebert et al., 1982) that luminal Ba^{++} addition, in the absence of luminal K^+, reduced G_e in a concentration-dependent manner, with a maximum reduction in G_e occurring at 5 mM luminal Ba^{++}.

The results shown in Fig. 9 indicate that the combination of luminal 5 mM Ba^{++}, zero K^+ produced a significant reduction in G_e, using either positive or negative current pulses; and that the electrical conductances returned to values indistinguishable from the control data when K^+ was restored, and Ba^{++} omitted, from luminal fluids. The data in Fig. 9 also indicate that, with lumi-

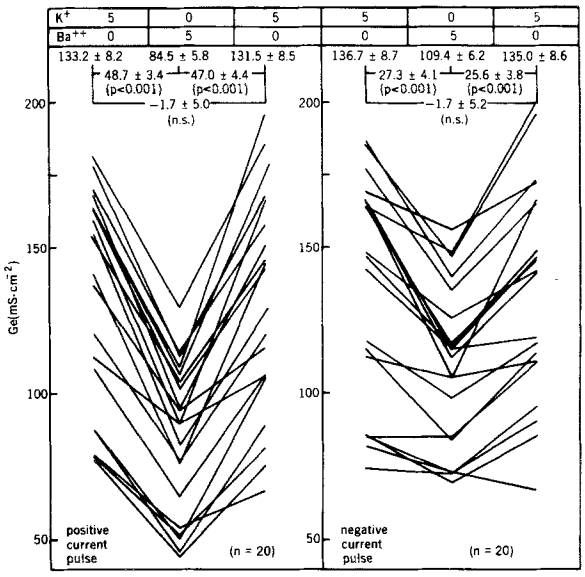

Fig. 9. The effect of combined 5 mM Ba^{++} addition and K^+ removal from luminal solutions on transepithelial conductance in paired experiments using both positive currents (left-hand panel) and negative currents (right-hand panel). The mTALH tubule segments were uniformly bathed with solutions containing ADH, 10 μU/ml. Each line connects measurements on individual tubules. The results are expressed as mean values ± SEM

nal 5 mM Ba^{++}, zero K^+, the ADH-dependent G_e fell to an appreciably greater extent with positive current pulses than with negative current pulses. Put differently, the reduction in G_e produced by luminal 5 mM Ba^{++}, zero K^+ was voltage-dependent; thus in the lower conductance state, but not the control state, the mouse mTALH exhibited significant electrical rectification.

The present experiments provide no information about the mechanism by which luminal zero K^+, 5 mM Ba^{++} produced electrical rectification in these tubule segments. However, this voltage dependence of the luminal 5 mM Ba^{++}, zero K^+ conductance effect is comparable to that observed by O'Neil (1983) and by Koeppen et al. (1983) in isolated rabbit cortical collecting tubules. It is also relevant to note in this context that, in excitable tissues, Ba^{++} is a blocker of K^+ channels (Eaton & Brodwick, 1980). Moreover, in excitable tissues, Armstrong, Swenson and Taylor (1982) have found that the probability of Ba^{++} blockade of a K^+ channel is greater for positive voltages oriented on the *cis* side of Ba^{++} solutions than when the latter are oriented voltage negative. The present data (Fig. 9) with luminal 5 mM Ba^{++}, zero K^+ are in qualitative accord with these findings of Armstrong et al.

Table 4. Effect of 0.1 mM luminal Ba^{++} on ADH-dependent G_e at varying luminal K^+ concentrations

Lumen K^+	Lumen Ba^{++}	G_e	ΔG_e (difference from control)	
(mM)		(mS cm^{-2})		
5	0	132.9 ± 21.0	Control	
0	0.1	98.4 ± 17.0	−34.4 ± 4.0	($P < 0.001$)
1	0.1	110.0 ± 18.8	−23.7 ± 2.5	($P < 0.001$)
5	0.1	121.7 ± 19.2	−11.6 ± 2.4	($P < 0.01$)
10	0.1	137.5 ± 19.5	+5.9 ± 3.0	(NS)
5	0	133.1 ± 17.8	+1.4 ± 3.8	(NS)
		[$n = 5$]		

Paired measurements of G_e were made in each of the indicated number of tubules with luminal solutions containing each of the indicated concentrations of K^+ and Ba^{++}. The luminal solutions were changed in the indicated sequence. ADH, 10 μU/ml, was uniformly present in the bath. The values of G_e are for positive luminal currents (*cf.* Fig. 9). The data are expressed as mean values ± SEM.

(1982). For convenience, the subsequent results on the effects of luminal Ba^{++} on G_e will be those obtained with positive luminal current pulses, in accord with the procedure reported by Koeppen et al. (1983).

Table 4 shows the results of paired experiments in which the ADH-dependent G_e was measured, using positive current pulses, with varying luminal concentrations of Ba^{++} and K^+. The combination of luminal 0.1 mM Ba^{++}, zero K^+ produced approximately a 25% reduction in G_e. Moreover, at a constant concentration of 0.1 mM Ba^{++} in luminal fluids, increases in luminal K^+ resulted in parallel increases in G_e so that, with luminal 10 mM K^+, 0.1 mM Ba^{++}, the G_e values were indistinguishable from control values. Thus it may be argued that the K^+/Ba^{++} luminal interactions were competitive in modifying G_e.

It was also appropriate to examine the effects of luminal 5 mM Ba^{++}, zero K^+ on the ADH-dependent permeability properties of the paracellular pathway to Na^+, which has a relatively high permeability coefficient and was the major ionic solute in external solutions. Thus we tested the effect of luminal zero K^+, 5 mM Ba^{++} on P_{Na}, as estimated from bath-to-lumen $^{22}Na^+$ fluxes, and on the Na^+/Cl^- permselectivity ratio, estimated from zero current NaCl dilution voltages. The control data in Table 5 indicate, in agreement with earlier studies (Hebert et al., 1981*a*), that the mouse mTALH was considerably more permselective to Na^+ than to Cl^-. The paired comparisons in Table 5 show that

Table 5. Effect of luminal K^- omission plus 5 mM luminal Ba^{++} addition on the ADH-dependent passive permeability properties of mTALH

Lumen		P_{Na}	P_{Na}/P_{Cl}
Ba^{++}	K^+		
(mM)		(μm sec^{-1})	(dilution voltage)
0	5	0.50 ± 0.07	4.2 ± 0.3
5	0	0.47 ± 0.05	4.6 ± 0.7
Mean paired difference		0.03 ± 0.06 (NS) [n = 4]	0.4 ± 0.4 (NS) [n = 5]

P_{Na} was determined from unidirectional $^{22}Na^+$ bath-to-lumen fluxes as described in Methods. The P_{Na}/P_{Cl} permselectivity ratio was determined, as described in Methods, from zero current bath dilution voltages. All observations involved paired comparisons on the indicated number of tubules. ADH, 10 μU/ml, was uniformly present in bathing solutions. All data were expressed as mean values ± SEM.

luminal 5 mM Ba^{++}, zero K^+ had no detectable effect either on P_{Na} or on the P_{Na}/P_{Cl} ratio.

It also seems improbable that the luminal 5 mM Ba^{++} and zero K^+ mediated reduction in the ADH-dependent value of G_e was referable to alterations in the K^+ conductance through the paracellular pathway. The following enabling calculations illustrate this argument. The tracer conductance of the i-th ion (g_i^l) through the paracellular route may be expressed as (Hodgkin, 1951)

$$g_i^l = \frac{P_i Z^2 F^2}{RT} [C_i] \tag{6}$$

where C_i is the mean concentration of the i-th ion in luminal and peritubular fluids. In the rabbit cTALH, Greger (1981*b*) found that the electrical P_K/P_{Na} ratio was approximately 1.3, and Work and Schafer (1982) noted that, in the rabbit mTALH, P_{Rb} determined from bath-to-lumen $^{84}Rb^+$ fluxes was 1.5×10^{-4} cm sec^{-1}, approximately twice as great as the tracer value for P_{Na} in that segment (Rocha & Kokko, 1973). In the mouse mTALH, the ADH-dependent value of P_{Na}, estimated from $^{22}Na^+$ fluxes, is approximately 0.5×10^{-4} cm sec^{-1} (*cf.* Table 5). Thus if one assumes that, in the mouse mTALH, P_K is twofold larger than P_{Na}, we have $P_K \cong 1.0 \times 10^{-4}$ cm sec^{-1}. By using the latter value together with the external solution K^+ concentrations of 5 mM used in the present experiments, Eq. (6) yields $g_K^l \cong 1.8$ mS cm^{-2}, about 20 fold smaller than the fall in G_e produced by luminal 5 mM Ba^{++}, zero K^+ with positive current injections (Fig. 9). Thus even if P_K were fourfold greater than P_{Na}, the K^+ conductance of the paracellular pathway would be too small, by about a factor of ten, to account for the fall in G_e produced by luminal 5 mM Ba^{++}, zero K^+.

In short, the combination of luminal 5 mM Ba^{++}, zero K^+ produced a reversible, voltage-dependent reduction in the ADH-dependent value of G_e (Fig. 9) and a reversible abolition of the long time-constant effect (Fig. 2). The luminal Ba^{++} effect on the ADH-dependent conductance could be reversed entirely by increasing luminal concentrations of K^+ (Table 6). The combination of luminal 5 mM Ba^{++}, zero K^+ had no detectable effect on the Na^+/Cl^- permselective characteristics of the paracellular pathway (Table 5); and in quantitative terms, the low concentrations of K^+ with respect to Na^+ in external solutions make it improbable that alterations in the K^+ conductance of the paracellular pathway referable to luminal Ba^{++}, zero K^+ could have accounted for the observed reductions in G_e (Fig. 9). When taken together, these observations are consistent with the possibility that apical membranes of the mTALH contained a significant Ba^{++}-sensitive K^+ conductance.

It is pertinent to consider whether ions other than K^+ also contributed to the conductance of apical plasma membranes. All the experiments reported in this paper were carried out in (CO_2 + HCO_3^-)-free solutions, so it is unlikely that HCO_3^- contributed to the measured values of G_e. It also seems improbable that these apical membranes contained Na^+ channels: V_e, and hence net Cl^- absorption, are insensitive to 10^{-3} M luminal amiloride (Hebert et al., 1981*a*); and, as indicated above, 10^{-3} M luminal amiloride did not affect G_e significantly. Likewise, since Cl^- removal from luminal solutions had no detectable effect on G_e (Table 1), any conductive pathway for Cl^- across apical membranes was small with respect to the Ba^{++}-sensitive apical membrane K^- conductance. These data, when taken together, are in accord with the hypothesis that K^+ was the major conductive species traversing apical membranes. Finally, these indirect arguments will be supported further by results obtained from cellular impalement studies presented in the companion manuscript (Hebert & Andreoli, 1984), namely, that luminal zero K^+, 5 mM Ba^{++} increased the ratio of apical to basolateral membrane resistance more than tenfold (*cf.* Table 1 in Hebert & Andreoli, 1984); and that zero-current K^+ dilution voltages across apical membranes of these tubules, estimated from cellular impalement experiments, yield an apical membrane K^+ transference number of approximately 0.87.

Consequently, the fall in G_e noted with positive

luminal current injections when luminal solutions were changed from control conditions to zero K^+, 5 mM Ba^{++} (Fig. 9) may be denoted as G_c^{min}, the minimal estimate of transcellular conductance. Obviously, G_c^{min} will be less than G_c if the Ba^{++} blockade of apical membrane K^+ channels was incomplete, or if other, unidentified ions had finite conductances through apical membranes. Accordingly, we may define G_s^{max}, the maximal estimate of paracellular conductance, as

$$G_s^{max} = G_e - G_c^{min}. \quad (7)$$

The ADH Effects on G_e, G_c^{min} and G_s^{max}

Table 6 summarizes the results of paired experiments in which G_e was measured with or without ADH in tubules exposed to luminal fluids containing either 5 mM K^+, zero Ba^{++} or zero K^+, 5 mM Ba^{++}. G_e was measured with positive luminal current injections; and paired measurements were made on each tubule for each condition. It should be noted that V_e and J_e were also measured in each tubule under each condition; for convenience, these latter data will be presented in Table 10.

The control data in Table 6 re-affirm the results in Figs. 4 and 5 and Table 2, namely, that ADH increased G_e in these tubules when luminal solutions contained 5 mM K^+, zero Ba^{++}. The values of G_s^{max} obtained with luminal 5 mM Ba^{++}, zero K^+, were statistically indistinguishable in the presence or absence of ADH. Moreover, the mean paired difference between G_c^{min} values with and without ADH was adequate to account quantitatively for the hormone-mediated increase in G_e. In other words, the results in Table 6 indicate that the ADH-dependent increase in transepithelial conductance was referable to an increase in transcellular rather than paracellular conductance. This latter observation is in keeping with earlier findings (Hebert et al., 1981*a*) that, in paired comparisons, ADH had no effect on two other ionic transport characteristics of the paracellular pathway, namely, P_{Na}, estimated from bath-to-lumen $^{22}Na^+$ fluxes, or on the electrical P_{Na}/P_{Cl} permselectivity ratio.

Effect of db-cAMP on Furosemide-Insensitive Net K^+ Secretion

It was also relevant to measure the effects of ADH, PGE_2 and db-cAMP on the rate of net K^+ secretion when luminal furosemide had reduced V_e to zero. The design of these experiments also derived from the following considerations.

Table 6. Effect of ADH on G_e, G_s^{max}, and G_c^{min}

ADH	G_e	G_s^{max}	G_c^{min}
		(mS cm^{-2})	
–	86.1 ± 9.0	68.9 ± 10.5	17.3 ± 3.4 ($P < 0.001$)
+	100.3 ± 7.9	64.4 ± 8.9	35.8 ± 3.6 ($P < 0.001$)
Mean paired difference (± ADH)	14.1 ± 2.1 ($p < 0.01$)	4.5 ± 4.6 NS	18.5 ± 4.0 ($P < 0.005$)
		[$n = 5$]	

Electrical conductances were measured in each of the experimental conditions in paired observations on each of the indicated number of tubules. G_e was measured under control conditions with 5 mM K^+, zero Ba^{++} in the lumen. G_s^{max} represents the conductances measured with luminal zero K^+, 5 mM Ba^{++}, G_c^{min} was calculated as the mean paired difference between G_e and G_s^{max} [Eq. (7)]. ADH, when present, was added to the bath at a concentration of 10 μU/ml. The results were expressed as mean values ± SEM. It should be noted that V_e and J_e were also measured in these tubules; for convenience, these latter data are presented in Table 10.

First, earlier findings (Culpepper & Andreoli, 1983) indicated that PGE_2 inhibits, in a seemingly competitive manner, ADH-mediated increments in V_e and J_{Cl}^{net} in the mTALH. More specifically, 10^{-6} M bath PGE_2 exceeds by tenfold the PGE_2 concentration required to abolish the increments in V_e and J_{Cl}^{net} produced by 10 μU/ml bath ADH, which is the lowest concentration of ADH producing a maximal enhancement of V_e and J_{Cl}^{net} (Hebert et al., 1981*a*; Culpepper & Andreoli, 1983). This PGE_2-mediated inhibition of Cl^- transport and V_e occurs at a pre-cAMP locus, since 10^{-6} M bath PGE_2 has no effect on the association constant between peritubular db-cAMP concentrations and db-cAMP-mediated increases in V_e and J_{Cl}^{net} (Culpepper & Andreoli, 1983). Moreover, 10^{-3} M bath db-cAMP, which is the lowest nucleotide concentration required for maximal stimulation of V_e and J_{Cl}^{net} (Hebert et al., 1981*a*), completely reverses the inhibition of V_e and J_{Cl}^{net} produced by 10^{-6} M bath PGE_2 in the presence of 10 μU/ml bath ADH (Culpepper & Andreoli, 1983).

Second, we found that 10^{-4} M luminal furosemide had no significant effect on the ADH-dependent value of G_c^{min}. Thus in five tubules, the ADH-dependent G_c^{min} was 57.6 ± 4.1 mS cm^{-2}, without furosemide, and 61.2 ± 4.7 mS cm^{-2}, with 10^{-4} M luminal furosemide; the difference between these two values was 3.6 ± 1.9 mS cm^{-2}, which was not statistically significant. Accordingly, it may be argued that furosemide did not interact with Ba^{++} in

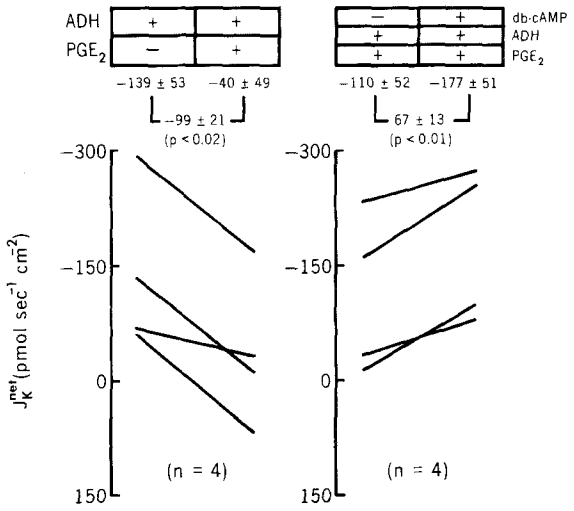

Fig. 10. Interactions between bath ADH (10 μU/ml), both prostaglandin E_2 (PGE_2, 10^{-6} M), and bath dibutyryl-cyclic AMP (db-cAMP, 10^{-3} M) on net K^+ secretion (J_K^{net}) in the presence of 10^{-4} M luminal furosemide. The tubule segments were perfused and bathed in symmetrical control solutions at 37°C. Each line connects measurements on individual tubules. With 10 μU/ml bath ADH and 10^{-4} M luminal furosemide, V_e was 0.4 ± 0.6 mV; all other values of V_e for the other conditions shown were also indistinguishable from zero. The data are expressed as mean values ± SEM

directly modulating the K^+ conductance of apical membranes.

Finally, we observed a detectable net rate of K^+ secretion when tubules were exposed to 10 μU/ml bath ADH and 10^{-4} M luminal furosemide, and V_e was indistinguishable from zero (Fig. 10). This result is not surprising, since Oberleitner, Guggino and Giebisch (1983) found that, in *Amphiuma* diluting segments obtained either from K^+-adapted or non-K^+-adapted animals, significant net K^+ secretion occurred in the presence of luminal furosemide, even when luminal solutions lacked Cl^-.

In the current experiments, we wished to evaluate whether, in the presence of luminal furosemide, PGE_2 inhibited net K^+ secretion occurring in the presence of ADH, and whether db-cAMP could reverse this inhibition. Thus we tested the interactions among 10^{-6} M bath PGE_2, 10 μU/ml bath ADH and 10^{-3} M bath db-cAMP on net K^+ secretion in tubules exposed to 10^{-4} M luminal furosemide. The results of these studies are presented in Fig. 10; as indicated in the legend to Fig. 10, V_e was indistinguishable from zero throughout all experiments. The left-hand panel of Fig. 10 shows that, in the presence of luminal furosemide and bath ADH, net K^+ secretion was present and that 10^{-6} M bath PGE_2 reduced by approximately 70% the furosemide-insensitive value of J_K^{net} which occurred in the presence of 10 μU/ml bath ADH. The results in the right-hand panel of Fig. 10 indicate that 10^{-3} M bath db-cAMP enhanced J_K^{net} significantly in the presence of 10 μU/ml bath ADH, 10^{-6} M bath PGE_2 and 10^{-4} M lumen furosemide.

Table 7. Effects of luminal zero K^+, 5 mM Ba^{++} on the ADH-dependent J_{Cl}^{net} and J_e

Luminal		J_i	ΔJ_i
		(pEq sec^{-1} cm^{-2})	
K^+	Ba^{++}		
		Net Cl^- flux (J_{Cl}^{net})	
5	0	8989 ± 1147	
			7998 ± 1207
			($P < 0.02$)
0	5	991 ± 292	
		($n = 3$)	
		Net electric flux (J_e)	
5	0	15,650 ± 1350	
			12,690 ± 1020
			($P < 0.001$)
0	5	2960 ± 450	
		($n = 20$)	

J_i (J_{Cl}^{net} in the upper top set of experiments; J_e in the bottom set of experiments) was measured in paired observations in each of the indicated numbers of tubules. ADH, 10 μU/ml, was present in the bathing solutions. The results are expressed as mean values ± SEM.

Relation of Luminal K^+/Ba^{++} Interactions with Net Cl^- Absorption

Table 7 lists the results of experiments in which we measured the effects of luminal 5 mM Ba^{++}, zero K^+ on the ADH-dependent values of J_i, expressed either as J_{Cl}^{net} (the upper part of Table 7) or as J_e (the lower part of Table 7). Both sets of experiments involved paired measurements on the indicated numbers of tubules; the choices of perfusion rates for J_{Cl}^{net} and J_e measurements were the same as described for Fig. 7.

The data shown in the upper part of Table 7 indicate that the combination of luminal 5 mM Ba^{++}, zero K^+ reduced J_{Cl}^{net} by approximately 89%. As indicated previously in connection with Table 6, these data indicate that the ADH-independent increase in G_c^{min} occurred when J_{Cl}^{net} was nearly abolished. The results listed in the lower half of Table 7 indicate that, with luminal 5 mM Ba^{++}, zero K^+, J_e fell by 81%. Thus there was a close relation between J_e and J_{Cl}^{net} both in the presence of luminal 5 mM Ba^{++}, zero K^+, just as was found in experiments without lumi-

Table 8. Effect of varying luminal K^+ on ADH-dependent J_e

Luminal K^+	J_e	ΔJ_e
(mM)	(pEq sec^{-1} cm^{-2})	
5	13,245 ± 2702	–
1	9630 ± 2248	3615 ± 554 ($P < 0.02$)
	($n = 3$)	
5	13,400 ± 2400	–
10	13,700 ± 2800	300 ± 800 (NS)
	($n = 5$)	

J_e was measured, in two sets of experiments, in paired comparisons in each of the indicated numbers of tubules. ADH, 10 μU/ml, was added to all bathing solutions. The values of ΔJ_e are with respect to the control data. The results are expressed as mean values ± SEM.

Table 9. Effect of 5 mM luminal Ba^{++} on ADH-dependent J_e

Luminal		J_e	ΔJ_e
K^+	Ba^{++}		
(mM)		(pEq sec^{-1} cm^{-2})	
5	0	15,328 ± 1290	Control
5	5	6,909 ± 812	8419 ± 536
5	0	14,076 ± 1339	1252 ± 720 (NS)
		[$n = 4$]	

J_e was measured, in the indicated sequence, in paired comparisons in each of the indicated number of tubules. ADH, 10 μU/ml, was added to all bathing solutions. The values of ΔJ_e are with respect to the control data. The results are expressed as mean values ± SEM.

nal zero K^+, 5 mM Ba^{++} (Fig. 7). Accordingly, we used J_e measurements as an index to the rate of net Cl^- absorption in tubules exposed to varying concentrations of either luminal K^+ or luminal Ba^{++}.

In order to evaluate the K^+ requirement for net Cl^- absorption in the mouse mTALH, we measured J_e in the presence of varying concentrations of luminal K^+ (Table 8). The data reported in the upper half of Table 8 indicate that reducing the luminal K^+ concentration from 5 to 1 mM reduced J_e significantly. Since the magnitude of the fall in J_e was nearly 10-fold greater than the measured rates of net K^+ secretion under a variety of experimental conditions (Figs. 8 and 10), the reduction in J_e produced by reducing luminal K^+ from 5 to 1 mM was due primarily to a fall in the rate of net Cl^- absorption. The data presented in the lower half of Table 8 indicate that increasing the luminal K^+ concentration from 5 to 10 mM had no detectable effect on J_e. These results are thus consistent with the possibility that, in the mouse mTALH, apical membrane Cl^- entry involved cotransport with K^+ and that maximal rates of apical membrane Cl^- entry occurred when the luminal K^+ concentrations were greater than 1 mM and less than or equal to 5 mM.

Table 9 presents the results of experiments that tested the effect of 5 mM luminal Ba^{++} on the ADH-dependent values of J_e. The luminal solutions contained 5 mM K^+, i.e., a luminal K^+ concentration that, from Table 8, was adequate to sustain maximal values for the ADH-dependent J_e. The results in Table 9 indicate that 5 mM luminal Ba^{++} resulted in approximately a 55% reduction in J_e. In other words, even in the presence of luminal 5 mM K^+, a Ba^{++}-mediated fall in apical membrane K^+ conductance reduced J_e, and hence presumably J_{Cl}^{net}.

Discussion

The experiments reported in this paper were designed to evaluate the effects of ADH on the electrical conductance of the isolated mouse mTALH, and the relations of these processes to hormone-mediated increments in the net rate of Cl^- absorption. Within the limits of experimental error, the following general conclusions appear permissible.

First, it is plausible to argue that K^+ was the primary conductive species traversing apical plasma membranes (Tables 1, 4, 5, and Fig. 9). Furthermore, the reduction in electrical conductance observed when control luminal solutions were replaced with those containing zero K^+, 5 mM Ba^{++} (Fig. 9) provided, as indicated in connection with Table 6, an estimate of G_c^{min}, the minimal conductance of the transcellular pathway.

Second, the ADH-dependent increase in G_e could be accounted for exclusively in terms of a hormone-dependent increase in G_c^{min} rather than in G_s^{max} [Table 6; Eq. (7)]. The ADH-dependent increase in G_c^{min} occurred under circumstances where luminal zero K^+, 5 mM Ba^{++} virtually abolished net Cl^- transport (Tables 6 and 7); therefore it is evident that ADH increased G_c^{min} even when net Cl^- absorption was absent. The results in Tables 2 and 3 indicate that ADH increased basolateral membrane Cl^- conductance, but only in concert with hormone-dependent increases in J_{Cl}^{net} [a mechanism for this Cl^- conductance increase will be considered in the companion paper (Hebert & Andreoli, 1984)]. Thus the hormone-dependent increase in G_c^{min} that occurred when net Cl^- transport was abolished (i.e., Table 6) may have been due to a hormone-dependent increase in apical membrane K^+ conductance, which is rate-limiting to total transcellular conductance either with or without hormone (Hebert & Andreoli,

1984). This argument, however, does not exclude the possibility that ADH might also have increased a non-Cl^- basolateral membrane conductance in the absence of net Cl^- transport.

Another set of results consistent with the view that ADH increased the K^+ conductance of apical membranes obtains from the observation that net K^+ secretion, which contributed about 10% to J_e (Fig. 8), was increased by db-cAMP in the presence of luminal furosemide, bath ADH, and bath PGE_2 (Fig. 10). Under the latter circumstances, V_e was virtually abolished (Fig. 7), so that there were no dissipative forces for net paracellular K^+ secretion. Consequently, the net rate of K^+ secretion increased either because db-cAMP increased the driving force for K^+ transport across apical membranes or because db-cAMP increased the K^+ conductance of apical membranes.

Now the results in the companion paper (Hebert & Andreoli, 1984) indicate that, with luminal 10^{-4} M furosemide, the apical membrane voltages are virtually the same with or without ADH. Furthermore, it seems unlikely that an increase in the cellular K^+ concentration could have accounted for the increase in net K^+ secretion produced by db-cAMP: the latter represented a 60% increment over the value of net K^+ secretion observed with bath ADH, bath PGE_2, and luminal furosemide (Fig. 10), and hence would have required a striking increase in the concentration of cellular K^+. But for an apical membrane dominated largely, if not exclusively, by a K^+ conductance (*cf.* above), such a result is inconsistent with the observation (Hebert & Andreoli, 1984) that, with furosemide, the apical membrane voltages were approximately the same with and without ADH. Thus the results in Fig. 10 are in accord with the view that db-cAMP increased the K^+ conductance of apical membranes.

Third, the fact that Cl^- removal from luminal solutions had no detectable effect on G_e (Table 1) permits a tentative conclusion about the relative conductive characteristics of the furosemide-sensitive apical membrane Cl^- entry process. Specifically, the results presented above, as well as in the companion paper (Table 1 in Hebert & Andreoli, 1984), indicate that K^+ was the major conductive species traversing apical membranes. When viewed in this context, the absence of detectable changes in G_e with luminal Cl^- deletion (Table 1) indicates that furosemide-sensitive apical membrane Cl^- entry had a negligibly small conductance with respect to apical membrane K^+ conductance. Furthermore, since J_e fell when luminal K^+ was reduced from 5 to 1 mM, it is plausible to argue that apical membrane Cl^- entry may have involved cotransport with both Na^+ and K^+. This conclusion is obviously in accord with the earlier suggestion of Greger (1981*a*) that, in the rabbit cTALH, apical Cl^- entry involves an electroneutral K^+, Na^+, $2Cl^-$ cotransport process.

Currents Through Apical Membranes and the Paracellular Pathway

Since cellular and paracellular pathways represent a parallel network, we have, for the open-circuit condition

$$i_s + i_c = 0 \tag{8a}$$

where i_s is the total current through the shunt and i_c is the total transcellular current. Since apical and basolateral membranes represent two conductive elements in series, it follows that

$$i_c = i_a = i_b \tag{8b}$$

where i_a and i_b are the total currents across apical and basolateral membranes, respectively.

The G_e values in Table 6 obtained in the presence of luminal zero K^+, 5 mM Ba^{++} provide an estimate to G_s^{max}, the maximal conductance of the shunt pathway [Eq. (7)]. Consequently, J_s^{max}, the maximal net electrical flux through the shunt pathway, may be computed as

$$J_s^{max} = i_s^{max}/F = G_s^{max}V_e/F \tag{9}$$

where i_s^{max} is the maximal total current through the shunt pathway.

Since control G_e values vary significantly among tubules (Figs. 6, 9), we carried out enabling calculations using Eqs. (8a), (8b) and (9) from a set of measurements in which all of the relevant data were obtained on the same set of tubules. Table 10 provides, using the paired data from Table 6, the calculated values of G_s^{max} and J_s^{max}; the V_e data and J_e values listed in Table 10 were obtained simultaneously with the other measurements listed in Table 6. It will be noted that the J_s^{max}/J_e ratios for these paired observations were: without ADH, 78.7%; and with ADH, 64.6%.

It is also noteworthy that entirely comparable values of J_s^{max}/J_e were computed from data including all tubules studied in the present experiments. The J_s^{max}/J_e ratio for the 11 tubules studied without ADH (in which G_e, G_c^{min}, V_e and J_e were measured simultaneously in each tubule; Fig. 6 and Table 6) was 57.5%; and for the 25 tubules studied with ADH (in which G_e, G_c^{min}, V_e and J_e were measured simultaneously in each tubule; Fig. 9 and Table 6), the J_s^{max}/J_e ratio was 63.7%.

Table 10. Calculation of G_s^{max}, J_s^{max}, and J_s^{max}/J_e

ADH	G_s^{max}	V_e	J_e	J_s^{max}	J_s^{max}/J_e
	(mS cm^{-2})	(mV)	(pEq sec^{-1} cm^{-2})		%
−	68.9 ± 10.5	5.4 ± 0.7	4800 ± 72	3778 ± 792	78.7
+	64.4 ± 8.9	9.1 ± 1.0	9410 ± 1237	6075 ± 1181	64.6
Mean paired difference	4.5 ± 4.6 NS	3.7 ± 1.0 ($P < 0.001$)	4609 ± 666 ($P < 0.001$)	2297 ± 511 ($P < 0.01$)	
		($n = 5$)			

The values of G_s^{max} are from Table 6. The values of V_e and J_e were measured simultaneously in the same tubules. J_s^{max} was calculated from Eq. (9). Data are expressed as mean values ± SEM.

The fact that the J_s^{max}/J_e ratios, either with or without ADH, were closely comparable also permits an enabling calculation of ${}^{Na}J_s^{max}$, the maximal net Na^+ flux of Na^+ through the paracellular pathway, as 0.8 J_s^{max}, since from Table 5 the shunt pathway was approximately four times more permeable to Na^+ than to Cl^-. Thus for ${}^{Na}J_s^{max} \cong 0.8\ J_s^{max}$, the data in Table 10 yield values of ${}^{Na}J_s^{max}/J_e$ of: 62.4%, without ADH; and 51.7%, with ADH. These results indicate that passive Na^+ absorption through the paracellular pathway amounted to approximately half of J_e, that is, the net rate of transcellular Cl^- absorption.

We now consider the currents across apical membranes. From Eqs. (8a), (8b) and (9), we have

$$i_a \leqq J_s^{max} F. \tag{10}$$

Now since the conductance of apical membrane Cl^- entry is negligible compared to apical membrane K^+ conductance (Tables 1, 6; Fig. 9), it is reasonable to consider that i_a was due predominantly to i_a^K, that is, K^+ efflux from cell to lumen through the Ba^{++}-sensitive pathway (Fig. 9). According to this view, we have

$$i_a \cong i_a^K \leqq J_s^{max} F. \tag{11}$$

A comparison of the J_s^{max} values in Table 10 with the ADH-dependent values of J_K^{net} (Fig. 8) indicates that the ratio J_K^{net}/J_s^{max} was approximately 0.1. Accordingly, about 90% or more of J_a^K may have recycled across apical plasma membranes, presumably through a Na^+, K^+ and Cl^- cotransport process in apical membranes. This analysis is in accord with the conclusions of other workers for coupled salt entry steps in similar epithelia (Greger, 1981*a*; Field et al., 1982; Halm et al., 1982; Greger & Schlatter, 1983*a*).

Figure 11 presents a schematic model for net Cl^- absorption in the mouse mTALH that summarizes these considerations. This model is similar to models proposed by other workers (Greger, 1981*a*; Murer & Greger, 1982; Oberleitner et al., 1982*a*,*b*, 1983) for Cl^- absorption in other renal tubular diluting segments having lumen-positive spontaneous transepithelial voltages. For convenience, Fig. 11 illustrates representative values for the ADH-dependent case, where V_e and J_{Cl}^{net} are generally about 10 mV, lumen positive, and approximately 10,000 pEq sec^{-1} cm^{-2}, respectively (Fig. 7; Table 10).

Given the calculations illustrated in Table 10, Fig. 11 indicates that approximately half of net Na^+ absorption occurred paracellularly. In other words, the combination of a lumen-positive V_e and a high shunt conductance reduced, with respect to exclusively transcellular, active Na^+ absorption, the metabolic energy expenditure for net Na^+ absorption. The remaining half of net Na^+ absorption is pictured as traversing a cellular route, presumably mediated via (Na^+ + K^+)-ATPase (Hebert et al., 1981*a*). Thus for a $3Na^+ : 2K^+$ stoichiometry of the latter, one-third of net transcellular Na^+ absorption was conductive. Accordingly, Fig. 11 indicates another, unidentified cation conductance, designated as J_+^b, across basolateral membranes.

Disparity between Tracer and Electrical Shunt Conductances

Table 10 indicates that G_s^{max}, the maximal electrical estimate of the shunt conductance, was 65–69 mS cm^{-2}. Now by using the P_{Na} and P_{Cl} values listed in Table 5 together with Eq. (6), we obtain a calculated tracer shunt conductance G_t of 34.3 mS cm^{-2}. Thus the calculated G_s/G_t ratio was 1.9–2.0. This result is consistent with the possibility (Hebert et al., 1981*a*) that ion transport through the paracellular shunt exhibited single-file behavior. Alternatively, G_s^{max} may have overestimated the shunt conductance, either because luminal zero K^+, 5 mM Ba^{++} did not en-

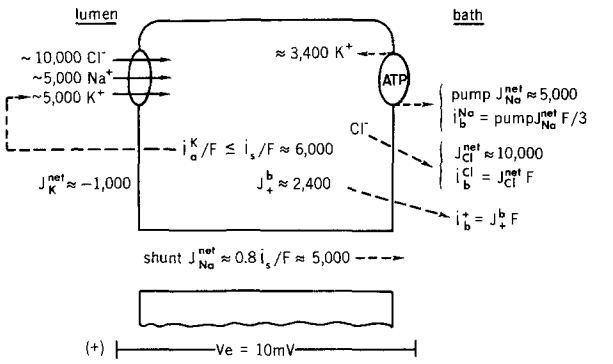

Fig. 11. Tentative model for NaCl absorption in the mouse mTALH. Conductive pathways are denoted by dashed arrows, and nonconductive pathways by solid arrows. All flux values are expressed as pEq sec^{-1} cm^{-2}. The symbols refer to the following: *pump* J^{net}_{Na}, net transcellular Na^+ absorption; i^{Na}_b, basolateral Na^+ current; i^{Cl}_b, conductive net Cl^- flux across basolateral membranes; J^b_+, presumed conductive cation flux from cell to bath; i^K_a, apical K^+ current; *shunt* J^{net}_{Na}, net paracellular Na^+ absorption; and J^{net}_K, net K^+ secretion. The value for J^{net}_K was obtained from the J^{net}_K/J^{net}_{Cl} ratio in Fig. 8 using J^{net}_{Cl} as 10,000 pEq sec^{-1} cm^{-2} for a V_e of 10 mV

tirely block apical membrane K^+ conductance units or because ions other than K^+ contributed significantly to apical conductance. Alternatively, if ions other than Na^+ and Cl^- had significant conductances through the paracellular pathway, the G_t term indicated above underestimated the true value of the shunt conductance. Evidently, additional studies are required to test these alternative possibilities explicitly.

The studies reported in this paper were supported by research grants from the National Institutes of Health (5 R01 AM-25540) and the National Science Foundation (PCM 81-41370), by an institutional grant from the National Institutes of Health (5 T32 AM-07408), and by an American Heart Grant-in-Aid (831294).

We acknowledge the able technical assistance of Ms. Jan Reid and Ms. Joanne Fusca and the able secretarial assistance of Ms. Linda Seidel and Ms. Clementine Whitman.

References

Armstrong, C.M., Swenson, R. P., Jr., Taylor, S.R. 1982. Block of squid axon K channels by internally and externally applied barium ions. *J. Gen. Physiol.* **80:**663–682

Burg, M.B., Isaacson, L., Grantham, J., Orloff, J. 1968. Electrical properties of isolated perfused rabbit renal tubules. *Am. J. Physiol.* **215:**788–794

Culpepper, R.M., Andreoli, T.E. 1983. Interactions among prostaglandin E_2 antidiuretic hormone and cyclic adenosine monophosphate in modulating Cl^- absorption in single mouse medullary thick ascending limbs of Henle. *J. Clin. Invest.* (*in press*)

Dunham, P.B., Stewart, G.W., Ellory, J.C. 1980. Chloride-activated passive potassium transport in human erythrocytes. *Proc. Natl. Acad. Sci. USA* **77:**1711–1715

Eaton, D.C., Brodwick, M.S. 1980. Effects of barium on the potassium conductance of squid axon. *J. Gen. Physiol.* **75:**727–750

Eveloff, J., Kinne, R. 1983. Sodium-chloride transport in the medullary thick ascending limb of Henle's loop: Evidence for a sodium-chloride cotransport system in plasma membrane vesicles. *J. Membrane Biol.* **72:**173–181

Field, M., Kimberg, L.S., Orellana, S.A., Frizzell, R.A. 1982. Potassium dependence of chloride transport in the intestine of the flounder *Pseudopleuronectes americanus*. *Bull. M. Desert Island Biol. Lab.* **21:**93–95

Geck, P., Pietrzyk, C., Burckhardt, B.-C., Pfeiffer, B., Heinz, E. 1980. Electrically silent cotransport of Na^+, K^+ and Cl^- in Ehrlich cells. *Biochim. Biophys. Acta* **600:**432–447

Good, D.W., Wright, F.S. 1979. Luminal influences on potassium secretion: Sodium concentration and fluid flow rate. *Am. J. Physiol.* **236:***F*192–*F*205

Greger, R. 1981*a*. Coupled transport of Na^+ and Cl^- in the thick ascending limb of Henle's loop of rabbit nephron. *Scand. J. Audiol.* **Suppl 14:**1–15

Greger, R. 1981b. Cation selectivity of the isolated perfused cortical thick ascending limb of Henle's loop of rabbit kidney. *Pfluegers Arch.* **390:**30–37

Greger, R., Schlatter, E. 1983*a*. Properties of the lumen membrane of the cortical thick ascending limb of Henle's loop of rabbit kidney. *Pfluegers Arch.* (*in press*)

Greger, R., Schlatter, E. 1983*b*. Properties of the basolateral membrane of the cortical thick ascending limb of Henle's loop of rabbit kidney. A model for secondary active chloride transport. *Pfluegers Arch.* (*in press*)

Guggino, W.B., Stanton, B.A., Giebisch, G. 1982. Regulation of apical potassium conductance in the isolated early distal tubule of the *Amphiuma* kidney. *Biophys. J.* **37:**338*a*

Hall, D.A., Varney, D.M. 1980. Effect of vasopressin on electrical potential difference and chloride transport in mouse medullary thick ascending limb of Henle's loop. *J. Clin. Invest.* **66:**792–802

Halm, D., Krasny, E., Frizzell, R. 1982. Apical membrane potassium conductance in flounder intestine: Relation to chloride absorption. *Bull. M. Desert Island Biol. Lab.* **21:**88–93

Hebert, S.C., Andreoli, T.E. 1984. The effects of antidiuretic hormone on cellular conductive pathways in mouse medullary thick ascending limbs of Henle. II. Determinants of the ADH-Mediated Increase in Transepithelial Voltage and in net Cl^- absorption. *J. Membrane Biol.* **80:**221–233

Hebert, S.C., Culpepper, R.M., Andreoli, T.E. 1981*a*. NaCl transport in mouse medullary thick ascending limbs. I. Functional nephron heterogeneity and ADH-stimulated NaCl cotransport. *Am. J. Physiol.* **241:***F*412–*F*431

Hebert, S.C., Culpepper, R.M., Andreoli, T.E. 1981*b*. NaCl transport in mouse medullary thick ascending limbs. II. ADH enhancement of transcellular NaCl cotransport; origin of the transepithelial voltage. *Am. J. Physiol.* **241:***F*432–*F*442

Hebert, S.C., Culpepper, R.M., Andreoli, T.E. 1981*c*. NaCl transport in mouse medullary thick ascending limbs. III. Modulation of the ADH effect by peritubular osmolality. *Am. J. Physiol.* **241:***F*443–*F*451

Hebert, S.C., Friedman, P.A., Andreoli, T.E. 1982. Cellular conductive properties of mouse medullary thick ascending limbs (mTALH). *Clin. Res.* **30:**449*a*

Hebert, S.C., Friedman, P.A., Andreoli, T.E. 1983. Vasopressin

(ADH) augments NaCl transport in mouse medullary thick limbs of Henle (mTALH) by increasing apical K^+ conductance and apical salt entry. *Clin. Res.* **31:**430*a*

Helman, S.I. 1972. Determination of electrical resistance of the isolated cortical collecting tubule and its possible anatomical location. *Yale J. Biol. Med.* **45:**339–345

Helman, S.I., Grantham, J.J., Burg, M. B. 1971. Effect of vasopressin on electrical resistance of renal cortical collecting tubules. *Am. J. Physiol.* **220:**1825–1832

Hodgkin, A.L. 1951. The ionic basis of electrical activity in nerve and muscle. *Biol. Rev.* **26:**339–409

Jacobson, A., Schwartz, M., Rehm, W.S. 1965. Effects of ambient alkaline earth concentrations of frog gastric secretion. *Physiologist* **8:**200

Kidder, G.W., III, Rehm, W.S. 1970. A model for the long time-constant transient voltage response to current in epithelial tissue. *Biophys. J.* **10:**215–236

Kielland, J. 1937. Individual activity coefficients of ions in aqueous solutions. *J. Am. Chem. Soc.* **59:**1675–1678

Koeppen, B.M., Biagi, B.A., Giebisch, G.H. 1983. Intracellular microelectrode characterization of the rabbit cortical collecting duct. *Am. J. Physiol.* **244:***F*35–*F*47

Lutz, M.D., Cardinal, J., Burg, M.B. 1973. Electrical resistance of renal proximal tubule perfused *in vitro*. *Am. J. Physiol.* **225:**729–734

Murer, H., Greger, R. 1982. Membrane transport in the proximal tubule and thick ascending limb of Henle's loop: Mechanisms and their alterations. *Klin. Wochenschr.* **60:**1103–1113

Oberleithner, H., Guggino, W., Giebisch, G. 1982*a*. Mechanism of distal tubular chloride transport in *Amphiuma* kidney. *Am. J. Physiol.* **242:***F*331–*F*339

Oberleithner, H., Giebisch, G., Lang, F., Wang, W. 1982*b*. Cellular mechanism of the furosemide sensitive transport system in the kidney. *Klin. Wochenschr.* **60:**1173–1179

Oberleithner, H., Guggino, W., Giebisch, G. 1983. The effect of furosemide on luminal sodium, chloride and potassium transport in the early distal tubule of *Amphiuma* kidney. Effects of potassium adaptation. *Pfluegers Arch.* (*in press*)

O'Neil, R.G. 1983. Voltage-dependent interaction of barium and cesium with the potassium conductance of the cortical collecting duct apical cell membrane. *J. Membrane Biol.* (*in press*)

Pacifico, A.D., Schwartz, M., MacKrell, N., Spangler, S.G., Sanders, S.S., Rehm, W.S. 1969. Reversal by potassium of an effect of barium on the frog gastric mucosa. *Am. J. Physiol.* **216:**536–541

Palfrey, H.C., Feit, P.W., Greengard, P. 1980. cAMP-stimulated cation cotransport in avian erythrocytes: Inhibition by "loop" diuretics. *Am. J. Physiol.* **238:***C*139–*C*148

Ramsey, J.A., Brown, R.H.J., Croghan, P.C. 1955. Electrometric titration of chloride in small volumes. *J. Exp. Biol.* **32:**822–829

Rocha, A.S., Kokko, J.P. 1973. Sodium chloride and water transport in the medullary thick ascending limb of Henle. *J. Clin. Invest.* **52:**612–622

Salling, N., Siggaard-Andersen, O. 1971. Liquid-junction potentials between plasma or erythrolysate and KCl solutions. *Scand. J. Clin. Lab. Invest.* **28:**33–40

Sasaki, S., Imai, M. 1980. Effects of vasopressin on water and NaCl transport across the *in vitro* perfused medullary thick ascending limb of Henle's loop of mouse, rat, and rabbit kidneys. *Pfluegers Arch.* **383:**215–221

Schafer, J.A., Troutman, S.L., Andreoli, T.E. 1974. Volume reabsorption, transepithelial potential differences, and ionic permeability properties in mammalian superficial proximal straight tubules. *J. Gen. Physiol.* **64:**582–607

Schultz, S.G., Frizzell, R.A, Nellans, H.N. 1977. An equivalent electrical circuit model for "sodium-transporting" epithelia in the steady-state. *J. Theor. Biol.* **65:**215–229

Shindo, T., Spring, K.R. 1981. Chloride movement across the basolateral membrane of proximal tubule cells. *J. Membrane Biol.* **58:**35–48

Work, J., Schafer, J.A. 1982. Rubidium transport in rat medullary thick ascending limb. *Proc. Am. Soc. Nephrol.* **15:**178*a*

Received 10 June 1983; revised 12 December 1983